



doi:10.7659/j.issn.1005-6947.2019.12.007
http://dx.doi.org/10.7659/j.issn.1005-6947.2019.12.007
Chinese Journal of General Surgery, 2019, 28(12):1482-1489.

· 基础研究 ·

药物诱导联合流出道狭窄构建兔腹主动脉瘤模型的实验研究

赵梦婕¹, 任玥颖¹, 胡璇¹, 孙安强², 陈增胜^{2,3}, 徐在品¹

(1. 贵州大学动物科学学院, 贵州 贵阳 550025; 2. 北京航空航天大学生物与医学工程学院, 北京 100083; 3. 北京航空航天大学生物医学工程高精尖创新中心, 北京 100083)

摘要

目的: 探讨药物诱导联合腹主动脉流出道狭窄构建兔腹主动脉瘤(AAA)模型的可行性与有效性。

方法: 将24只雌性新西兰大白兔随机均分为4组, 其中两组分别采用含CaCl₂(0.75 mol/L)或胰蛋白酶(0.04 g/mL)溶液的棉条包裹浸润血管30 min诱导AAA, 另两组分别在CaCl₂或胰蛋白酶浸润的基础上行腹主动脉流出道狭窄术(狭窄50%~60%)造模。术后使用超声诊断仪监测受累血管管径变化, 术后2周, 收集损伤段腹主动脉制作组织切片行HE与EVG染色。用计算机模拟评估流出道狭窄对AAA形成的影响。

结果: 术后2周, 超声检查显示, 两个单纯药物浸润组受累血管扩张不明显, 均未达到AAA形成标准, 两个药物联合狭窄组受累血管明显扩张, 其中CaCl₂+狭窄组成瘤率66.67%(4/6), 血管平均扩张1.61倍; 胰蛋白酶+狭窄组成瘤率83.33%(5/6), 血管平均扩张1.89倍。与正常腹主动脉比较, CaCl₂浸润的血管内膜厚度明显增加(均P<0.05), 而胰蛋白酶浸润后的血管内膜厚度变化不明显(均P>0.05); 各组中膜厚度均明显增加, 弹力纤维面积百分比均明显降低, 其中CaCl₂+狭窄组的变化最为明显(均P<0.05)。计算机数值模拟结果显示, 流出道狭窄后血管壁应力增大, 成瘤率增加。

结论: 药物损伤联合腹主动脉流出道狭窄能成功构建兔AAA模型, 缩短造模时间, 且胰蛋白酶浸润损伤联合腹主动脉流出道狭窄造模方法优于CaCl₂联合腹主动脉流出道狭窄造模方法。

关键词

主动脉瘤, 腹; 模型, 动物; 兔

中图分类号: R654.3

Experimental study of construction of rabbit abdominal aortic aneurysm model by drug induction combined with outflow coarctation

ZHAO Mengjie¹, REN Yueying¹, HU Xuan¹, SUN Anqiang², CHEN Zengsheng^{2,3}, XU Zaipin¹

(1. College of Animal Science, Guizhou University, Guiyang 550025, China; 2. School of Biological and Medical Engineering, Beihang University, Beijing 100083, China; 3. Biomedical Engineering High-tech Innovation Center, Beihang University, Beijing 100083, China)

Abstract

Objective: To investigate the feasibility and effectiveness of creating rabbit abdominal aortic aneurysm (AAA) model by using drug induction plus abdominal aortic outflow coarctation.

Methods: Twenty-four female New Zealand white rabbits were equally randomized into 4 groups, in which,

基金项目: 国家自然科学基金资助项目(11862004; 11872096); 黔科合平台人才基金资助项目([2018]5781)。

收稿日期: 2019-09-29; **修订日期:** 2019-11-12。

作者简介: 赵梦婕, 贵州大学动物科学学院硕士研究生, 主要从事宠物医学与实验外科学方面的研究。

通信作者: 徐在品, Email: 368462323@qq.com

AAA model was induced by wrapping and infiltrating the vessel with a cotton strip containing a solution of CaCl_2 (0.75 mol/L) or trypsin (0.04 g/mL) in two groups, and the model was constructed by CaCl_2 or trypsin infiltration plus abdominal aorta outflow constriction (50% 60% constriction) in the other two groups. After the operation, the change in diameter of the affected blood vessel was monitored by veterinary ultrasound. The experimental animals were sacrificed 2 weeks after the operation, and the injured abdominal aorta was harvested to prepare tissue sections for HE and EVG staining. The effect of outflow tract coarctation on AAA formation was evaluated by computer simulation.

Results: Ultrasound examination on 2 weeks after operation showed that no evident dilatation of the affected vessel was seen, and no vessel reached the standard of AAA formation in the two groups undergoing drug infiltration alone; the affected vessel was obviously dilated in the two group undergoing drug infiltration plus abdominal aortic outflow coarctation, in which, the AAA formation rate was 66.67% (4/6) in CaCl_2 plus coarctation group, with an average 1.61-fold expansion, and the AAA formation rate was 83.33% (5/6) in trypsin plus coarctation group, with an average 1.89-fold expansion. Compared with the normal abdominal aorta, the thickness of abdominal aorta intima was significantly increased after CaCl_2 infiltration (both $P < 0.05$), but the thickness of abdominal aorta intima did not significantly change after trypsin infiltration (both $P > 0.05$); the thickness of the tunica media was significantly increased and the percentage of the area occupied by the elastic fibers was significantly reduced in all groups, and these changes were most evident in CaCl_2 plus coarctation group (all $P < 0.05$). Computer numerical simulation demonstrated that the vascular wall stress increased and the AAA formation rate increased after the outflow coarctation.

Conclusion: Drug induction plus abdominal aortic outflow coarctation can successfully establish the AAA model in rabbits, and shorten the time for model generation. Moreover, the modelling method of trypsin infiltration combined with abdominal aortic outflow coarctation is superior to that of CaCl_2 infiltration combined with abdominal aortic outflow coarctation.

Key words Aortic Aneurysm, Abdominal; Models, Animal; Rabbits

CLC number: R654.3

腹主动脉瘤 (abdominal aortic aneurysms, AAA), 是指腹主动脉的某一段的异常扩张或局限性膨胀, 最终使得管壁无法承受血流冲击而破裂的一种高危性疾病, 当扩张的腹主动脉直径超过正常腹主动脉直径 1.5 倍以上时即可诊断为 AAA^[1]。该病目前尚无可靠的治疗方法, 可选择的仅有开放修复术 (open repair) 或介入修复 (endovascular aortic aneurysm repair, EVAR)^[2-3], 这两种主动干预措施对患者而言都是昂贵且危险的^[4-5]。为寻找潜在的治疗方案, 必须对 AAA 的发生和发展加以理解, 而动物模型是用于研究 AAA 发生和发展机制的重要工具。过去常用的 AAA 动物模型再现了炎症、弹力纤维降解、细胞外基质的破坏和主动脉扩张^[6]等被预测为人类主动脉瘤发展的决定因素。2016 年, Crawford 等^[7]发现小直径 AAA 的破裂或与流出道阻塞有关, 这意味着除了腹主动脉结构的破坏以外, 其壁面压应力的改变

同样影响 AAA 的形成和发展。基于此, 本实验通过药物浸润破坏动脉壁结构联合腹主动脉流出道狭窄增大血管壁面压应力, 观察不同药物、不同压力下 AAA 形成时间及血管病理变化的差异。

1 材料与方法

1.1 试剂与仪器

无水氯化钙 (CaCl_2) (生工生物工程上海股份有限公司); 1:250 胰蛋白酶 (生工生物工程上海股份有限公司); 普通外科器械包 (上海医疗器械集团有限公司手术器械厂); SSW-3 显微外科器械包 (上海医疗器械集团有限公司手术器械厂); 猫用导尿管 (古氏贸易上海有限公司, 规格 1.0/1.3); VINNO 6 兽用彩超诊断仪 (飞依诺科技苏州有限公司); 犬眠宝 (青岛汉河动植物药业有限公司)。

1.2 试验动物与分组

健康新西兰大白兔24只,雌性,体质量2~3 kg,随机分为4组,每组6只,AAA造模方法分别采用CaCl₂浸润(CaCl₂组)、CaCl₂浸润联合流出道缩窄(CaCl₂+缩窄组)、胰蛋白酶浸润(胰蛋白酶组)、胰蛋白酶浸润联合流出道缩窄(胰蛋白酶+缩窄组)。

1.3 试验方法

1.3.1 AAA模型的制备 肌肉注射犬眠宝进行全身麻醉(0.1 mL/kg),仰卧固定,术部无菌准备。取脐下腹白切口,切开腹腔后用无菌纱布将肠管包裹推向腹腔上方及右侧,显露腹主动脉及伴行的腔静脉^[8]。显微镊钝性分离肾下腹主动脉前壁、侧壁、后壁脂肪组织及其与腔静脉之间间隙,游离出肾动脉水平以下髂动脉水平以上腹主动脉段约1 cm,以游标卡尺测量血管直径。分别用宽1 cm,浸有0.75 mol/L CaCl₂溶液或0.04 g/mL胰蛋白酶溶液的棉条包裹游离的腹主动脉段,再用等宽橡皮条包裹棉条,以保护腔静脉及周围组织。30 min后去除棉条及橡皮条,生理盐水反复冲洗3次,以防周围组织粘连。药物+缩窄组根据血管直径,选择型号1.0(直径0.075 cm)或1.3(直径0.105 cm)的猫导尿管于浸润段远心端同腹主动脉平行结扎,后撤出导尿管,使之形成约50%~60%的缩窄。逐层关腹,术后连续使用青霉素3 d(40万U/只)。

1.3.2 彩超诊断仪检测 术后每周使用VINNO 6兽用彩超诊断仪,F4-12L探头,将频率调至3.2 MHz,对实验兔进行腹主动脉超声检查,观察并测量浸润段腹主动脉直径变化。

1.3.3 组织病理学观察 2周后,牺牲实验兔,取腹主动脉损伤段固定、包埋、切片,分别行HE染色观察主动脉壁组织结构及细胞组成变化、EVG染色观察动脉瘤管壁弹力纤维破坏的程度。使用CaseViewer软件于扫描图上每组各取10处测量内膜、中膜厚度,取平均值。每组内每张切片挑选3个200倍视野进行拍照,应用Image-Pro Plus 6.0软件分别对每张照片测量黑色弹力纤维面积和视野内组织总面积,并求出各个视野的弹力纤维比。

1.3.4 计算机模拟血管壁应力 假设血液为牛顿流体,密度为1 060 kg/m³^[7],动态黏度为2.18 mPa·s^[9],假设每单位时间进入肾下主动脉的血流量是恒定的并且等于0.12 L/min^[10],输入腹主动脉术前直径、狭窄后直径和成瘤后直径,使用ANSYS 15.0模拟

AAA并计算不同情况下腹主动脉管壁所受峰值应力(peak wall stress, PWS)。

1.4 统计学处理

各组数据均用均数±标准差($\bar{x} \pm s$)表示,应用Excel和SPSS 19.0软件进行数据统计学处理,组间比较用Duncan法检验, $P < 0.05$ 为差异有统计学意义。

2 结果

2.1 AAA超声图像及各组直径、成瘤率比较

造模2周后,各组均无实验兔死亡。CaCl₂组损伤段血管管壁呈强回声影像、管壁增厚,血管直径与未损伤段对比略有扩张;CaCl₂+缩窄组血管明显扩张,呈梭形;胰蛋白酶组管径较未损伤段略有扩张,管壁无明显增厚;胰蛋白酶+缩窄组损伤段血管显著扩张,管壁变薄,较CaCl₂+缩窄组瘤体形态更圆(图1)。两个单纯药物组血管扩张均未达1.5倍,无AAA形成;CaCl₂+缩窄组4只(4/6)成瘤,血管平均扩张1.61倍;胰蛋白酶+缩窄组5只(5/6)成瘤,血管平均扩张1.89倍。胰蛋白酶+缩窄组成瘤率及血管扩张倍数均大于CaCl₂+缩窄组(表1)。

2.2 组织病理学观察

正常腹主动脉结构由内向外依次为内膜、内弹性膜(呈波浪状,为内、中膜分界线)、中膜(主要为中层平滑肌细胞和弹力纤维)、外膜,HE染色可见血管壁结构清晰,中膜平滑肌排列整齐,无明显炎性细胞浸润,EVG染色示弹力纤维完整连续,层次清晰,曲度明显,内膜极薄;CaCl₂组HE染色可见外膜炎性细胞浸润,管壁正常结构破坏,EVG染色示内膜增厚,内弹性膜曲度变直,中膜弹力纤维出现断裂、碎片;CaCl₂+缩窄组HE染色见外膜炎性细胞浸润,中膜层结构严重破坏,EVG染色见内弹力膜与内膜分离,形成腔隙,中膜层裂解;胰蛋白酶组HE染色见管壁结构无明显变化,有炎性细胞浸润,EVG染色示内膜增厚,弹力纤维结构完整,原有曲度改变,仍可见连续性;胰蛋白酶+缩窄组HE染色见管壁结构疏松,平滑肌细胞排列紊乱,有炎性细胞浸润,EVG染色示弹力纤维层次不清,可见断裂、变细及空泡形成(图2)。

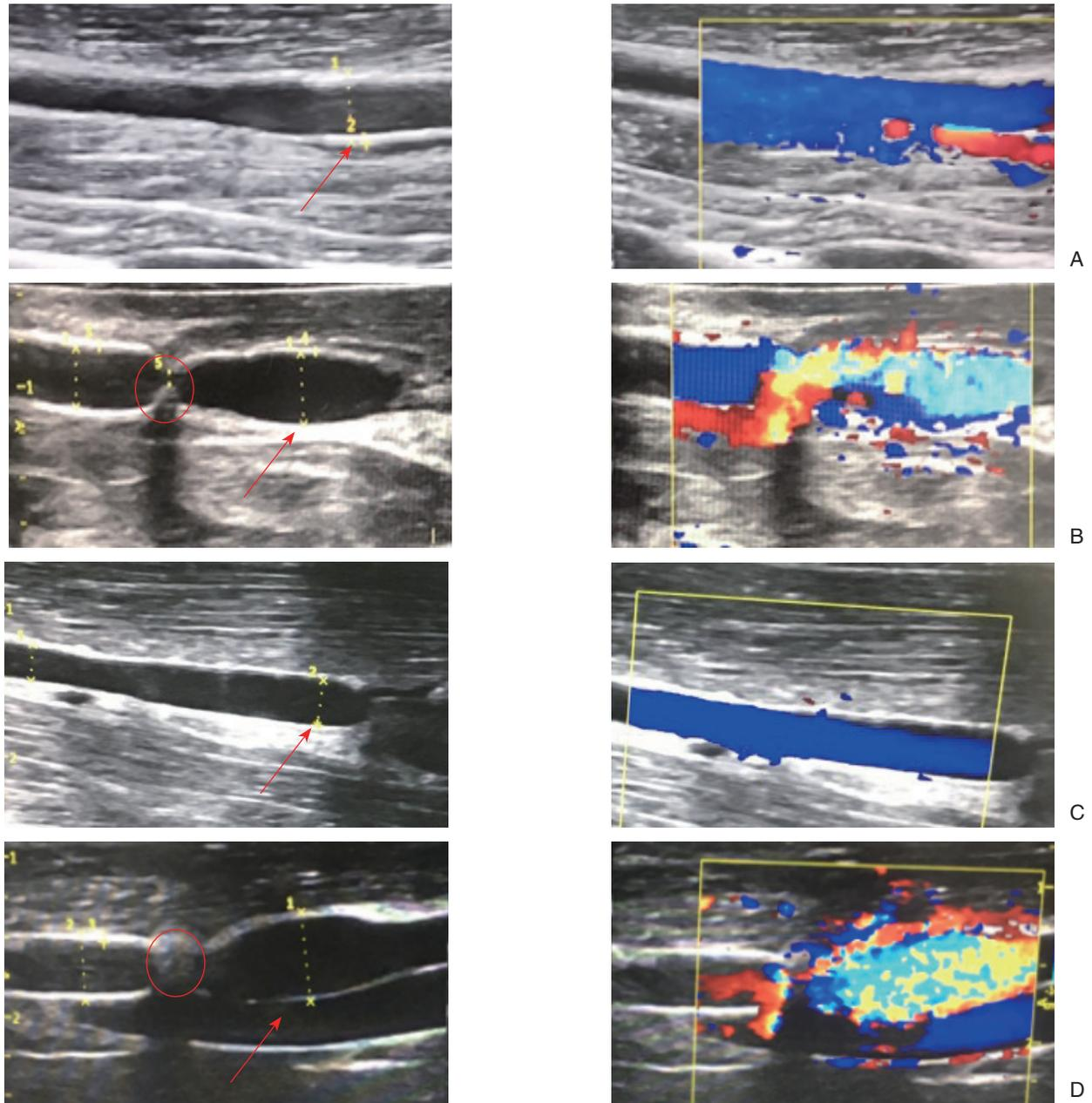


图 1 腹主动脉超声图像 (血流方向均为从右向左, 箭头指向为药物损伤段; 圈内为动脉缩窄处) A: CaCl₂ 组; B: CaCl₂+ 缩窄组; C: 胰蛋白酶组; D: 胰蛋白酶 + 缩窄组

Figure 1 Ultrasound image of the abdominal aorta (the right-to-left direction of blood flow, the arrow showing the drug injured segment, and inside the circle showing the coarctation of abdominal aorta) A: CaCl₂ group; B: CaCl₂ plus coarctation group; C: Trypsin group; D: Trypsin plus coarctation group

表 1 各组腹主动脉直径变化及成瘤率比较 (n=6)

Table 1 Comparison of diameter changes and AAA formation rates of abdominal aorta in each group (n=6)

组别	术前直径 (cm, $\bar{x} \pm s$)	术后 2 周最大直径 (cm, $\bar{x} \pm s$)	扩张倍数 (倍)	成瘤 [n (%)]
CaCl ₂ 组	0.18 ± 0.05	0.27 ± 0.01	1.47	0 (0.00)
CaCl ₂ + 缩窄组	0.23 ± 0.06	0.37 ± 0.04	1.61	4 (66.67)
胰蛋白酶组	0.22 ± 0.03	0.27 ± 0.04	1.31	0 (0.00)
胰蛋白酶 + 缩窄组	0.19 ± 0.05	0.36 ± 0.02	1.89	5 (83.33)

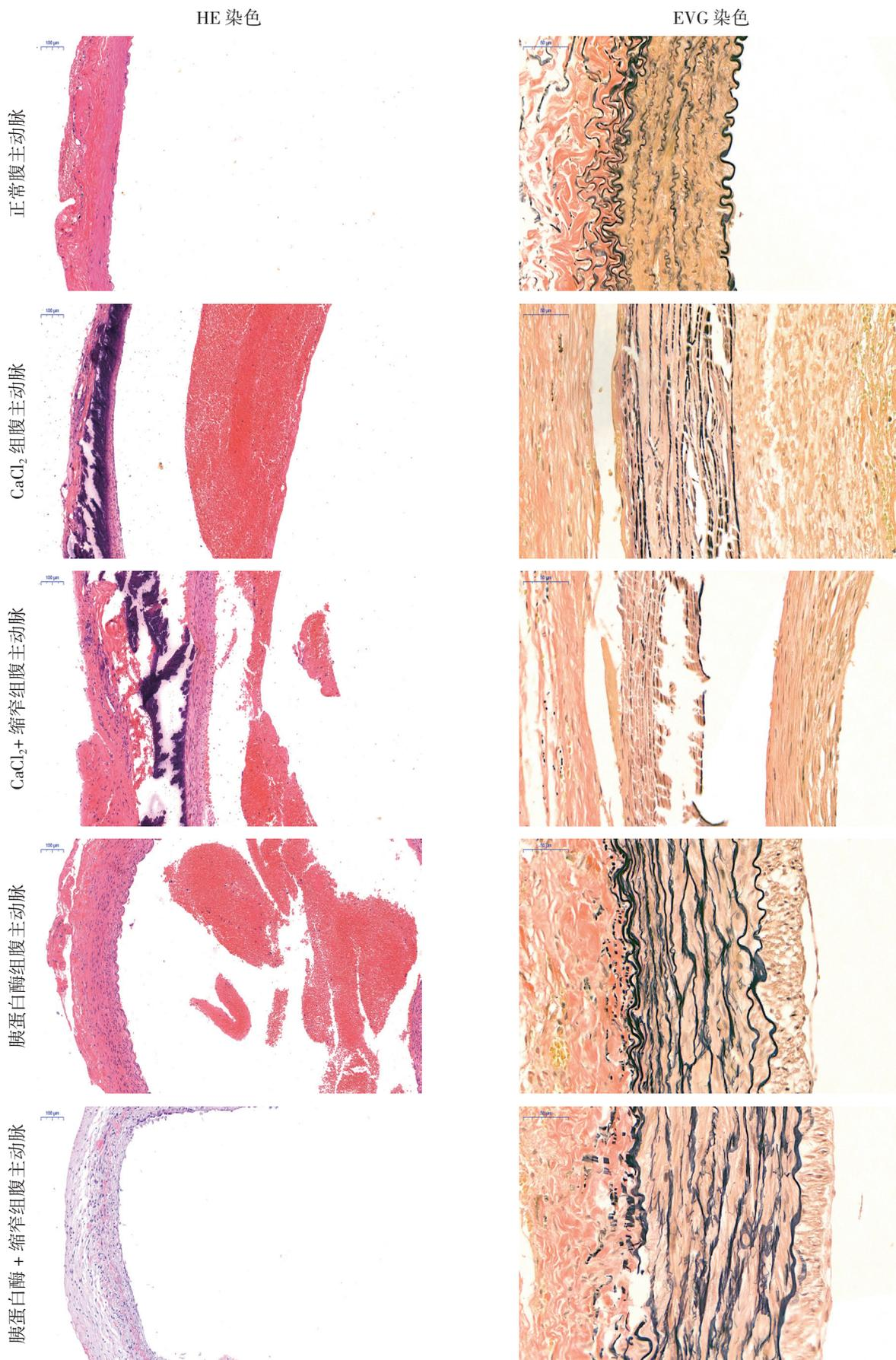


图 2 腹主动脉 HE (×100; 标尺: 100 μm)、EVG (×400; 标尺: 50 μm) 染色结果
Figure 2 HE (×100; scale bar: 100 μm) and EVG (×400; scale bar: 50 μm) staining results of abdominal aorta

2.3 内膜、中膜厚度及各组弹力纤维面积百分比变化

正常腹主动脉内膜厚度约为3.2 μm, 药物损伤使血管内膜增厚, 且CaCl₂损伤后的血管内膜厚度明显大于胰蛋白酶损伤后的血管(均P<0.05)。正常腹主动脉血管中膜厚度约为134.83 μm, CaCl₂组与CaCl₂+缩窄组中膜较正常腹主动脉增厚33.65%、150.14%, 且均明显高于胰蛋白酶组与胰蛋白酶+缩窄组(均P<0.05); 胰蛋白酶组与胰蛋白酶

酶+缩窄组中膜厚度较正常腹主动脉增加10.68%、13.55%, 但差异无统计学意义(均P>0.05)。正常腹主动脉弹力纤维面积约为血管总面积的41.48%, 药物损伤后各组弹力纤维面积百分比比较正常腹主动脉均明显降低(均P<0.05), 相同药物组间差异不明显(均P>0.05), CaCl₂组明显低于胰蛋白酶组, 与胰蛋白酶+缩窄组差异不明显(P>0.05); CaCl₂+缩窄组明显低于胰蛋白酶组与胰蛋白酶+缩窄组(P<0.05)(表2)。

表 2 腹主动脉壁厚度变化及各组弹力纤维面积百分比 (n=6, $\bar{x} \pm s$)

Table 2 Changes in vessel wall thickness of abdominal aorta and percentage of elastic fiber area in each group (n=6, $\bar{x} \pm s$)

参数	正常腹主动脉	CaCl ₂ 组	CaCl ₂ +缩窄组	胰蛋白酶组	胰蛋白酶+缩窄组
内膜(μm)	3.20 ± 1.00	91.20 ± 8.18 ¹⁾	91.60 ± 4.59 ¹⁾	77.73 ± 5.33	58.20 ± 5.20
中膜(μm)	134.83 ± 5.68	180.23 ± 13.27 ¹⁾	337.27 ± 21.72 ¹⁾	153.10 ± 3.03 ¹⁾	149.23 ± 7.05 ¹⁾
弹力纤维面积百分比(%)	41.48 ± 13.11	5.37 ± 0.82 ¹⁾	2.80 ± 0.70 ¹⁾	24.21 ± 3.06 ¹⁾	15.59 ± 3.38 ¹⁾

注: 与正常腹主动脉比较, P<0.05

Note: P<0.05 vs. normal abdominal aorta

2.4 计算机模拟血管壁面压应力

正常状态下血管壁面压应力约为13.342 kPa (1 mmHg=0.133 kPa), 将腹主动脉流出道缩窄后, 缩窄处近心端的血管壁面压应力增大为13.397 kPa;

成瘤后, 流出道未缩窄的AAA壁面压应力约为13.384 kPa, 而流出道缩窄的AAA壁面压应力约为13.436 kPa(图3)。

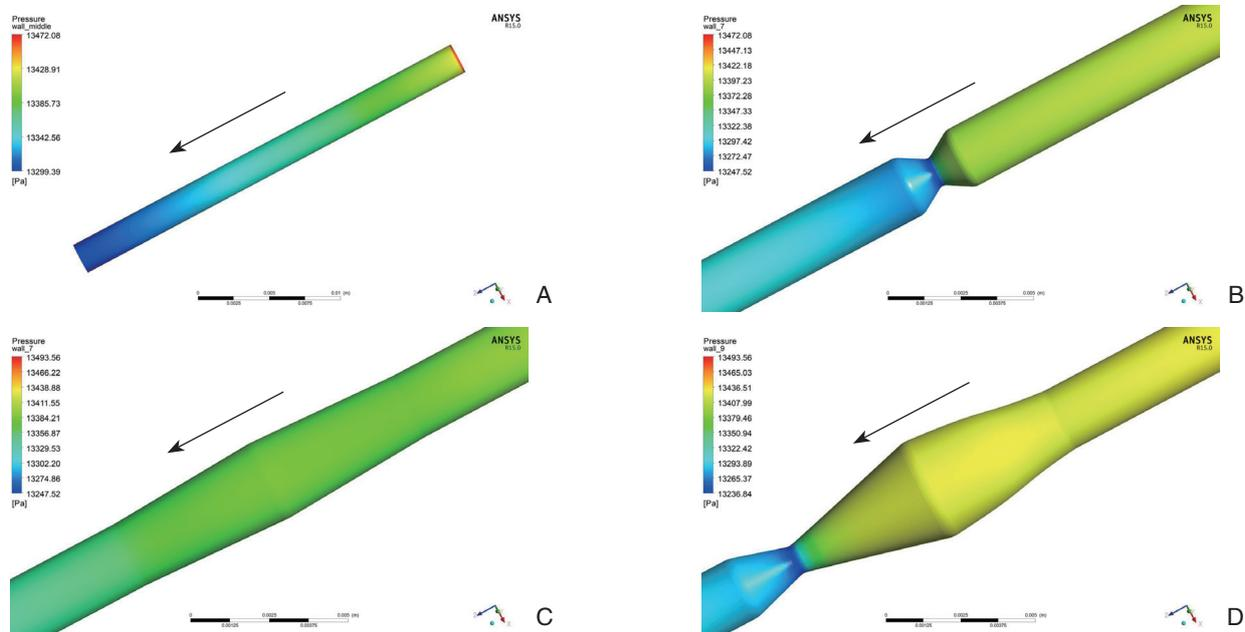


图 3 缩窄与未缩窄的腹主动脉壁面压应力示意图(箭头指向为血流方向) A: 正常腹主动脉; B: 缩窄后的腹主动脉; C: 流出道未缩窄的 AAA; D: 流出道缩窄后形成的 AAA

Figure 3 Wall pressure stress of abdominal aorta with coarctation and without coarctation (arrow showing the direction of blood flow) A: Normal abdominal aorta; B: Abdominal aorta with coarctation; C: AAA without outflow coarctation; D: AAA with outflow coarctation

3 讨论

AAA是一种动脉退行性疾病,多发生于65岁以上人群^[11-12]。在AAA形成中有4个主要过程:蛋白水解,氧化应激,炎症免疫反应和血管平滑肌细胞(VSMC)凋亡,每次脉动后导致动脉壁弹性和阻力丧失并阻碍正常动脉直径恢复的过程^[13]。

钙化是人体AAA的特征之一,约80%的AAA都显示相当大程度的主动脉壁钙化^[14]。1988年Gertz等^[15]使用CaCl₂应用于兔颈动脉外膜诱导动脉瘤形成,3周后,与对侧颈动脉相比,用CaCl₂处理的动脉段管腔直径平均增加了61%,组织学检查显示,动脉扩张伴有弹性蛋白钙化,VSMC缺失,炎性细胞明显浸润,这是人类动脉瘤新模型的第一份报告,其作用机制在于沉积的钙盐与弹性蛋白结合,直接破坏弹性纤维层;钙盐可以损伤内皮细胞,促进炎性细胞浸润,分泌基质金属蛋白酶降解弹性纤维,从而导致腹主动脉扩展,形成AAA。Freestone等^[16]在1997年发表的研究中用0.25 mol/L CaCl₂作用于新西兰兔腹主动脉,术后12周内未诱导AAA形成;2001年Chiou等^[17]用0.68 mol/L CaCl₂应用于C57 BL/6小鼠的腹主动脉10 min,手术后3周形成AAA;2011年张明芳等^[18]用0.75 mmol/L CaCl₂溶液包裹浸润腹主动脉,于术后6周直径扩张124.12%。本实验使用0.75 mol/L CaCl₂溶液作用于兔腹主动脉,联合动脉流出道缩窄,于术后2周使其动脉扩张达原来的1.61倍。

1990年,Anidjars等^[19]首次通过灌注弹性蛋白酶诱导兔肾下AAA,由于其病理生理状态较符合人类AAA特征,如内侧弹性蛋白退化和外膜巨噬细胞浸润等^[20],成为AAA的经典模型之一。弹性蛋白酶具有破坏大动脉中层弹性蛋白结构的特性,此法也用于大鼠、犬^[21]、猪^[22]的AAA模型中,在这些研究中,均发现了如内膜增厚、中膜弹性层受损和破碎、中膜和外膜明显的炎性浸润等特征。本实验从外膜包裹浸润,使胰蛋白酶渗透进而消化中膜弹力层,同样观察到上述病理变化,相较传统的胰蛋白酶灌注法,本实验操作简便易行,术后2周血管扩张达1.89倍。

Laplace定律和最大AAA直径长期用于指导AAA破裂的风险评估和选择修复的阈值建议^[23],最新的美国和欧洲对AAA的临床实践指南建议对AAA直径 ≥ 5.5 cm的无症状患者进行修复^[24-25],但这一标准过于单一且准确性不高,有报道^[26-27]显示,通过研究AAA的生物力学或结构特征可有助于

提高破裂预测的准确性。有研究证明流出道阻塞的AAA与普通AAA相比PWS显著增高^[7],当PWS超过主动脉壁强度时,AAA极有可能发生破裂^[28]。通过计算机模拟发现,流出道缩窄同样使成瘤前后的血管壁应力增大,因此将流出道缩窄与药物损伤联合,通过增大PWS加速血管扩张,在相同时间、相同条件下,缩窄后的血管获得直径更大的AAA。这意味着通过药物损伤联合腹主动脉流出道缩窄可以在更短的时间内获得AAA,为研究提供便利。

总之,药物损伤联合腹主动脉流出道缩窄能成功构建兔AAA模型,缩短造模时间,胰蛋白酶浸润联合流出道缩窄造模效果优于CaCl₂浸润联合流出道缩窄造模,且较符合临床AAA特征。

参考文献

- [1] Johnston KW, Rutherford RB, Tilson MD, et al. Suggested standards for reporting on arterial aneurysms. Subcommittee on Reporting Standards for Arterial Aneurysms, Ad Hoc Committee on Reporting Standards, Society for Vascular Surgery and North American Chapter, International Society for Cardiovascular Surgery[J]. *J Vasc Surg*, 1991, 13(3):452-458. doi: 10.1067/mva.1991.26737.
- [2] Lindholt J S, Søgaard R, Laustsen J. Prognosis of ruptured abdominal aortic aneurysms in Denmark from 1994-2008[J]. *Clin Epidemiol*, 2012, 4:111-113. doi: 10.2147/CLEP.S31098.
- [3] Chen ZG, Tan SP, Diao YP, et al. The long-term outcomes of open and endovascular repair for abdominal aortic aneurysm: A meta-analysis [J]. *Asian J Surg*, 2019, 42(10):899-906. doi: 10.1016/j.asjsur.2019.01.014.
- [4] Lindholt JS, Juul S, Fasting H, et al. Hospital costs and benefits of screening for abdominal aortic aneurysms. Results from a randomised population screening trial[J]. *Eur J Vasc Endovasc Surg*, 2002, 23(1):55-60. doi: 10.1053/ejvs.2001.1534.
- [5] Greenleaf EK, Hollenbeak CS, Aziz F. Outcomes after ruptured abdominal aortic aneurysm repair in the era of centralized care[J]. *J Vasc Surg*, 2019, pii: S0741-5214(19)31781-1. doi: 10.1016/j.jvs.2019.06.187. [Epub ahead of print]
- [6] Lysgaard Poulsen J, Stubbe J, Lindholt JS. Animal Models Used to Explore Abdominal Aortic Aneurysms: A Systematic Review[J]. *Eur J Vasc Endovasc Surg*, 2016, 52(4):487-499. doi: 10.1016/j.ejvs.2016.07.004.
- [7] Crawford JD, Chivukula VK, Haller S, et al. Aortic outflow occlusion predicts rupture of abdominal aortic aneurysm[J]. *J Vasc Surg*, 2016, 64(6):1623-1628. doi: 10.1016/j.jvs.2016.03.454.
- [8] 吕瑜环, 龚万和, 徐在品, 等. 犬假体腹主动脉瘤的制作[J]. *中国普通外科杂志*, 2011, 20(12):1327-1330.

- Lu YH, Gong WH, Xu ZP, et al. Creation of a prosthetic abdominal aortic aneurysm in dogs[J]. Chinese Journal of General Surgery, 2011, 20(12):1327-1330.
- [9] 王春艳, 童庭辉, 丁玉辉, 等. 机械通气下静脉全身麻醉对兔血液黏度和红细胞流变性的影响[J]. 现代预防医学, 2011, 38(13):2543-2544.
- Wang CY, Tong TH, Ding YH, et al. The influence of intravenous general anaesthesia on hemorheology of rabbit undergoing mechanical ventilation[J]. Modern Preventive Medicine, 2011, 38(13):2543-2544.
- [10] 万广志, 管静芝, 宋祖军, 等. 乌司他丁对百草枯中毒致兔肾损伤的保护作用[J]. 中国药物应用与监测, 2013, (5):265-267. doi:10.3969/j.issn.1672-8157.2013.05.008.
- Wan GZ, Guan JZ, Song ZJ, et al. Protective effects of ulinastatin on kidney damage induced by paraquat poisoning in rabbit[J]. Chinese Journal of Drug Application and Monitoring, 2013, (5):265-267. doi:10.3969/j.issn.1672-8157.2013.05.008.
- [11] George J, Rapsomaniki E, Pujades-Rodriguez M, et al. How Does Cardiovascular Disease First Present in Women and Men? Incidence of 12 Cardiovascular Diseases in a Contemporary Cohort of 1,937,360 People[J]. Circulation, 2015, 132(14):1320-1328. doi: 10.1161/CIRCULATIONAHA.114.013797.
- [12] Laine MT, Vanttinen T, Kantonen I, et al. Rupture of Abdominal Aortic Aneurysms in Patients Under Screening Age and Elective Repair Threshold[J]. Eur J Vasc Endovasc Surg, 2016, 51(4):511-516. doi: 10.1016/j.ejvs.2015.12.011.
- [13] Torres-Fonseca M, Galan M, Martinez-Lopez D, et al. Pathophysiology of abdominal aortic aneurysm: biomarkers and novel therapeutic targets[J]. Clin Investig Arterioscler, 2019, 31(4):166-177. doi: 10.1016/j.arteri.2018.10.002.
- [14] Maier A, Gee MW, Reeps C, et al. Impact of calcifications on patient-specific wall stress analysis of abdominal aortic aneurysms[J]. Biomech Model Mechanobiol, 2010, 9(5):511-521. doi: 10.1007/s10237-010-0191-0.
- [15] Gertz SD, Kurgan A, Eisenberg D. Aneurysm of the rabbit common carotid artery induced by periarterial application of calcium chloride in vivo[J]. J Clin Invest, 1988, 81(3):649-656. doi: 10.1172/JCI113368.
- [16] Freestone T, Turner RJ, Higman DJ, et al. Influence of hypercholesterolemia and adventitial inflammation on the development of aortic aneurysm in rabbits[J]. Arterioscler Thromb Vasc Biol, 1997, 17(1):10-17. doi: 10.1161/01.atv.17.1.10.
- [17] Chiou AC, Chiu B, Pearce WH. Murine aortic aneurysm produced by periarterial application of calcium chloride[J]. J Surg Res, 2001, 99(2):371-376. doi: 10.1006/jsre.2001.6207.
- [18] 张明芳, 陈锋, 朱仙花, 等. 兔腹主动脉瘤模型的建立[J]. 中国普通外科杂志, 2011, 20(6):605-608.
- Zhang MF, Chen F, Zhu XH, et al. Establishment of abdominal aortic aneurysm model in rabbits[J]. Chinese Journal of General Surgery, 2011, 20(6):605-608.
- [19] Anidjar S, Salzmann JL, Gentric D, et al. Elastase-induced experimental aneurysms in rats[J]. Circulation, 1990, 82(3):973-981. doi: 10.1161/01.cir.82.3.973.
- [20] Pyo R, Lee JK, Shipley JM, et al. Targeted gene disruption of matrix metalloproteinase-9 (gelatinase B) suppresses development of experimental abdominal aortic aneurysms[J]. J Clin Invest, 2000, 105(11):1641-1649. doi: 10.1172/JCI8931.
- [21] Furubayashi K, Takai S, Jin D, et al. The significance of chymase in the progression of abdominal aortic aneurysms in dogs[J]. Hepatol Res, 2007, 30(4):349-357. doi: 10.1291/hypres.30.349.
- [22] Czerski A, Bujok J, Gnus J, et al. Experimental methods of abdominal aortic aneurysm creation in swine as a large animal model[J]. J Physiol Pharmacol, 2013, 64(2):185-192.
- [23] Maier A, Gee MW, Reeps C, et al. A comparison of diameter, wall stress, and rupture potential index for abdominal aortic aneurysm rupture risk prediction[J]. Ann Biomed Eng, 2010, 38(10):3124-3134. doi: 10.1007/s10439-010-0067-6.
- [24] Chaikof EL, Dalman RL, Eskandari MK, et al. The society for vascular surgery practice guidelines on the care of patients with an abdominal aortic aneurysm[J]. J Vasc Surg, 2018, 67(1):2-77. doi: 10.1016/j.jvs.2017.10.044.
- [25] Wanhainen A, Verzini F, Van Herzele I, et al. Editor's Choice-European Society for Vascular Surgery (ESVS) 2019 Clinical Practice Guidelines on the Management of Abdominal Aorto-iliac Artery Aneurysms[J]. Eur J Vasc Endovasc Surg, 2019, 57(1):8-93. doi: 10.1016/j.ejvs.2018.09.020.
- [26] Barrett HE, Cunnane EM, Hidayat H, et al. On the influence of wall calcification and intraluminal thrombus on prediction of abdominal aortic aneurysm rupture[J]. J Vasc Surg, 2018, 67(4):1234-1246. doi: 10.1016/j.jvs.2017.05.086.
- [27] Man V, Polzer S, Gasser TC, et al. Impact of isotropic constitutive descriptions on the predicted peak wall stress in abdominal aortic aneurysms[J]. Med Eng Phys, 2018, 53:49-57. doi: 10.1016/j.medengphy.2018.01.002.
- [28] Soto B, Vila L, Dilmé JF, et al. Increased Peak Wall Stress, but Not Maximum Diameter, Is Associated with Symptomatic Abdominal Aortic Aneurysm[J]. Eur J Vasc Endovasc Surg, 2017, 54(6):706-711. doi: 10.1016/j.ejvs.2017.09.010.

(本文编辑 宋涛)

本文引用格式: 赵梦婕, 任玥颖, 胡璇, 等. 药物诱导联合流出道缩窄构建兔腹主动脉瘤模型的实验研究[J]. 中国普通外科杂志, 2019, 28(12):1482-1489. doi:10.7659/j.issn.1005-6947.2019.12.007

Cite this article as: Zhao MJ, Ren YY, Hu X, et al. Experimental study of construction of rabbit abdominal aortic aneurysm model by drug induction combined with outflow coarctation[J]. Chin J Gen Surg, 2019, 28(12):1482-1489. doi:10.7659/j.issn.1005-6947.2019.12.007